Study of the structural and phase state of ceramics synthesized from 6YSZ - Al_2O_3 – HfO_2 by semi–dry pressing followed by sintering in vacuum

M. Abilev[1,2], D. Yerbolat[1*], M. Skakov[1], Al. Zhilkashinova[1], A. Pavlov[1,3], N. Kantay[1], S. Gert[4], As. Zhilkashinova[1], L. Łatka[5]

[1]S. Amanzholov East Kazakhstan University, Ust-Kamenogorsk, Kazakhstan
[2]Al-Farabi Kazakh National University, Almaty, Kazakhstan
[3]"KAZ CERAMICS" LLP, Ust-Kamenogorsk, Kazakhstan
[4]Center of Excellence VERITAS, D. Serikbaev East Kazakhstan Technical University, Ust-Kamenogorsk, Kazakhstan
[5]Wroclaw University of Science and Technology, Wroclaw, Poland
[*]E-mail: *diaserbolat16@gmail.com*

The study investigates the properties of 6YSZ – Al_2O_3 – HfO_2 powder mixture and the resulting ceramics obtained by semi-dry pressing followed by sintering in vacuum. X-ray fluorescence spectrometry revealed the primary constituents as zirconium (81%), aluminum (8.7%), yttrium (5.7%), and hafnium (3.5%). The average particle diameter was 0.5 μm, with specific surface area and bulk weight recorded at 18,535 cm^2/g and 0.84 g/cm^3, respectively. X-ray phase analysis indicated a predominance of monoclinic zirconium dioxide. Sintering at 1400-1600°C transformed the phase composition, enhancing density and microhardness, with values peaking at 5.8 g/cm^3 and 12.1 GPa at 1600°C. This process also increased the tetragonal phase content to 63%. The ceramics exhibited the highest crack resistance at 1600°C, attributed to the stabilized tetragonal zirconium dioxide. Microstructural analysis confirmed the homogenous distribution of the elements and the presence of fine fractions influencing microstructural properties. 1600°C was found to be the optimal temperature for sintering the 6YSZ – Al_2O_3 – HfO_2 ceramics.

Keywords: composite ceramics; zirconium oxide; semi-dry pressing; structural-phase state; sintering.

Жартылай құрғақ престеу және вакуумда күйдіру әдісімен алынған 6YSZ-Al_2O_3 – HfO_2 керамиканың құрылымдық-фазалық күйін зерттеу

М. Абилев[1,2], Д. Ерболат[1*], М. Скаков[1], Ал. Жилкашинова[1], А. Павлов[1,3], Н. Кантай[1], С. Герт[4], Ас. Жилкашинова[1], Л. Латка[5]

[1]С. Аманжолов атындағы Шығыс Қазақстан университеті, Өскемен қ., Қазақстан
[2]Әл-Фараби атындағы Қазақ ұлттық университеті, Алматы қ., Қазақстан
[3]"KAZ CERAMICS" ЖШС, Өскемен қ., Қазақстан
[4]"VERITAS" артықшылық орталығы, Д. Серікбаев атындағы Шығыс Қазақстан техникалық университеті, Өскемен қ., Қазақстан
[5]Вроцлав ғылым және технологиялар университеті, Вроцлав қ., Польша
[*]E-mail: *diaserbolat16@gmail.com*

Бұл мақалада 6YSZ – Al_2O_3 – HfO_2 ұнтақ қоспасының және жартылай құрғақ престеуден кейінгі вакуумдық күйдіру арқылы алынған керамиканың қасиеттері зерттелді. Рентгендік флуоресценциялық спектрометрия көмегімен негізгі компоненттер анықталды: цирконий (81%), алюминий (8,7%), иттрий (5,7%) және гафний (3,5%). Бөлшектердің орташа диаметрі 0,5 мкм, ал меншікті бетінің ауданы мен массалық тығыздығы сәйкесінше 18535 $см^2/г$ және 0,84 $г/см^3$ болды. Рентгендік фазалық талдау моноклинді цирконий диоксидінің басым екенін көрсетті. 1400-1600°C температурада күйдіру тығыздық пен микроқаттылықты 5,8 $г/см^3$ және 12,1 ГПа 1600°C максималды мәндерге дейін арттыра отырып, фазалық құрамын өзгертті. Бұл процесс тетрагональды фазаның құрамын 63%-ға дейін арттырды. Керамика тұрақтандырылған тетрагональды цирконий диоксидіне байланысты 1600°C температурада ең жоғары жарыққа төзімділікті көрсетті. Микроқұрылымдық талдау элементтердің біртекті таралуын және микроқұрылымдық қасиеттерге әсер ететін шағын фракциялардың болуын растады. 6YSZ – Al_2O_3 – HfO_2 керамикасын күйдіру үшін оңтайлы температура 1600°C болатыны анықталды.

Түйін сөздер: композициялық керамика; цирконий оксиді; престеу; физикалық-механикалық қасиеттері; құрылымы**.**

Исследование структурно-фазового состояния 6YSZ – Al_2O_3 – HfO_2 керамики, синтезированной методом полусухого прессования с последующим спеканием в вакууме

М. Абилев[1,2], Д. Ерболат[1*], М. Скаков[1], Ал. Жилкашинова[1], А. Павлов[1,3], Н. Кантай[1], С. Герт[4], Ас. Жилкашинова[1], Л. Латка[5]

[1]Восточно-Казахстанский университет им. С. Аманжолова, г. Усть-Каменогорск, Казахстан
[2]Казахский национальный университет им. аль-Фараби, г. Алматы, Казахстан
[3]ТОО "KAZ CERAMICS", г. Усть-Каменогорск, Казахстан
[4]Центр превосходства "VERITAS", Восточно-Казахстанский технический университет им. Д. Серикбаева, г. Усть-Каменогорск, Казахстан
[5]Вроцлавский университет науки и технологий, г. Вроцлав, Польша
[*]E-mail: *diaserbolat16@gmail.com*

В статье изучены свойства порошковой смеси 6YSZ – Al_2O_3 – HfO_2 и керамики, полученной полусухим прессованием с последующим спеканием в вакууме. Рентгенофлуоресцентная спектрометрия выявила основные компоненты: цирконий (81%), алюминий (8,7%), иттрий (5,7%) и гафний (3,5%). Средний диаметр частиц составил 0,5 мкм, а удельная поверхность и насыпная масса зафиксированы на уровне 18535 $см^2/г$ и 0,84 $г/см^3$ соответственно. Рентгенофазовый анализ показал преобладание моноклинного диоксида циркония. Спекание при 1400-1600°C изменило фазовый состав, повысив плотность и микротвердость до максимальных значений 5,8 $г/см^3$ и 12,1 ГПа при 1600°C. Этот процесс также увеличил содержание тетрагональной фазы до 63%. Керамика показала наибольшую трещиностойкость при 1600°C, обусловленную стабилизированным тетрагональным диоксидом циркония. Микроструктурный анализ подтвердил однородное распределение элементов и наличие мелких фракций, влияющих на микроструктурные свойства. Установлено, что оптимальной температурой для спекания керамики 6YSZ – Al_2O_3 – HfO_2 является 1600°C.

Ключевые слова: композиционная керамика; оксид циркония; полусухое прессование; структурно-фазовое состояние; спекание.

(2024) Chem Bull Kaz Nat Univ 3:12-21

CHEMICAL BULLETIN
of Kazakh National University
http://bulletin.chemistry.kz/

IRSTI: 31.17.15; 61.35.29 https://doi.org/10.15328/cb1375

Article

Study of the structural and phase state of ceramics synthesized from 6YSZ - Al_2O_3 – HfO_2 by semi–dry pressing followed by sintering in vacuum

M. Abilev[1,2], D. Yerbolat[1]*, M. Skakov[1], Al. Zhilkashinova[1], A. Pavlov[1,3], N. Kantay[1], S. Gert[4], As. Zhilkashinova[1], L. Łatka[5]

[1]S. Amanzholov East Kazakhstan University, 34 Tridtsatoy Gvardeiskoy Divizii Str., 070002 Ust-Kamenogorsk, Kazakhstan
[2]Al-Farabi Kazakh National University, al-Farabi Ave. 71, 050040 Almaty, Kazakhstan
[3]"KAZ CERAMICS" LLP, Obyezdnoe Highway 5/2, F06C4T3 Ust-Kamenogorsk, Kazakhstan
[4]Center of Excellence VERITAS, D. Serikbaev East Kazakhstan Technical University, D. Serikbayev Str. 19, 070004 Ust-Kamenogorsk, Kazakhstan
[5]Wroclaw University of Science and Technology, Wybrzeże Stanisława Wyspiańskiego 27, 50-370 Wroclaw, Poland
*E-mail: *diaserbolat16@gmail.com*

1. Introduction

High-tech ceramics based on zirconium dioxide (ZrO_2) are used in various technological fields due to their unique physical and mechanical properties and precise structural control. Main applications include dentistry, orthopedics, chemical and metallurgical industries, fuel cells, and oxygen sensors. The properties of zirconium ceramics are largely determined by their phase composition and microstructure [1-5].

The phase composition of ZrO_2-based ceramics can be controlled by alloying ZrO_2 with heterovalent metal oxides and applying special heat treatments. For example, yttrium oxide (Y_2O_3) stabilizes the tetragonal phase of ZrO_2 at room temperature by matching the trivalency and ionic radius (Y^{3+}, 1.06 Å) with Zr^{4+} (0.87 Å). This alloying produces sintered ceramics with over 90% of the t-ZrO_2 phase [5-11].

Hafnium oxide (HfO_2), a structural analogue of ZrO_2, can also be used to modify ceramic properties. HfO_2 exists in monoclinic, tetragonal, and cubic forms, with similar lattice parameters to ZrO_2. The ZrO_2-HfO_2 system can form solid solutions due to their identical ionic radii and valence. Tetragonal HfO_2, stabilized with Y_2O_3, is stable above 1770°C, while the cubic phase, having a longer bond length, is more suitable for stabilization [12-14].

Sintering ZrO_2–Al_2O_3 ceramics in a vacuum at 1450-1600°C increases density and stabilizes the phases, producing materials with high mechanical strength and thermal stability. The composite material consisting of 6YSZ (yttria-stabilized zirconia or a mixture of ZrO_2 powder doped with 6 mol% Y_2O_3 powder), Al_2O_3, and HfO_2 shows superior properties, making it suitable for aerospace engines, cutting tools, wear-resistant coatings, and high-temperature reactors [15-17].

Recent studies have focused on tailoring the microstructure of 6YSZ–Al_2O_3–HfO_2 composites using advanced fabrication techniques such as hot pressing. These methods achieve dense, homogeneous composites with controlled grain sizes and enhanced properties.

Hot pressing sintering is a widely used technique in the fabrication of advanced ceramics. It combines the application of heat and uniaxial pressure to densify powders into a solid, coherent structure. This method is particularly advantageous for materials that are difficult to sinter using conventional techniques due to their high melting points or poor diffusion rates [18-21].

Hot pressing sintering is a powerful technique for producing high-quality ceramic materials with superior mechanical properties and controlled microstructures. By leveraging the combined effects of heat and uniaxial pressure, this method addresses the limitations of conventional sintering and meets the demands of advanced technological applications. As the field of materials science continues to evolve, hot pressing sintering will remain a critical process in the development of next-generation ceramic components [20, 21].

Received 23 May 2024; Received in revised form 12 Aug 2024; Accepted 28 Aug 2024; Available online 08 Oct 2024.

As research advances, composite ceramics are expected to play a crucial role in next-generation technologies. Developing sintering additives based on transition metal oxides is essential to reduce sintering temperatures and simplify manufacturing processes while controlling the structure of the resulting ceramics.

The aim of the current study is to synthesize composite ceramics based on yttrium-stabilized zirconium dioxide (6YSZ), aluminum and hafnium oxides by semi-dry pressing and vacuum sintering, and to investigate the structure and physico-chemical properties of the resulting materials.

2. Experiment

Initial powders were Y_2O_3-stabilized ZrO_2 (6YSZ, 99.9%, CAS No. 114168-16-0), Al_2O_3 (99.95%, CAS No. 1344-28-1) and HfO_2 (≥99.95%, CAS No. 12055-23-1). 6YSZ powder particles are diamond-shaped crystals with a size of up to 10 μm. Al_2O_3 powder particles have a predominantly elongated shape (up to 10 μm in length). HfO_2 particles have a shape closer to round, the average particle size is 1.3 μm.

The powders were mixed in the following proportion: 85 wt.% 6YSZ + 10 wt.% Al_2O_3 + 5 wt. % HfO_2. This composition was chosen based on a series of experiments studying the effect of adding Al_2O_3 and HfO_2 stabilizers on the processes of structural transformation of zirconium oxide with a change in symmetry from monoclinic to tetragonal m-ZrO_2 → t-ZrO_2 [22, 23].

AUM210-E electronic analytical scales with an accuracy of 0.0001 g were used to measure the mass of used powders during the experiment and analyses. The powders were dried in a drying cabinet SPU-80-01 with an accuracy of maintaining a set temperature of ± 1°C. The press mass was prepared with the addition of an organic binder based on a 10% solution of polyvinyl alcohol mixed with a plasticizer - glycerin in a ratio of 7:3. The amount of the introduced organic binder in terms of the formation of granules of the press powder was 10 wt.%.

The forming of blanks from the resulting press mass was carried out by uniaxial semi-dry pressing on ES0501 hydraulic press, with a pressing force of 98-118 MPa and exposure at maximum pressure for 30 seconds. The molded products had dimensions: diameter 13.0 mm, thickness 3.0 – 3.5 mm.

The organic binder was burned out in an oxidizing environment at 1200°C using a SNOL 400/12-VP electric furnace (VNIIETO, Russia), accuracy of maintaining the temperature was ±5°C. The final sintering of the products was carried out in an electric vacuum chamber furnace SNVE-1.3.1/20 (Prizma LLC, Russia), the vacuum depth was $1.1 \cdot 10^{-2}$ Pa. The ceramics were sintered in three modes:

1) heating to 1400°C → holding for 2 h;

2) heating to 1500°C → holding for 2 h;

3) heating to 1600°C → holding for 2 h.

The crystal structure of powders and sintered samples was studied using an XPertPRO diffractometer (Malvern Analytical Empyrean, Netherlands) using monochromatized copper X-ray diffraction with a scan step of 0.03° (Kα1 [Å] 0.1542). A measurement angle of 20-100°, X-ray tube voltage of 40 kV, current of 30 mA, measurement time at each step was 10 s, and an aluminum rectangular multi-purpose sample holder (PW1172/01) were used. Quantitative analysis of the phase composition and structure of the samples was carried out using additional analysis software HighScore Plus and Powder Cell.

The study of the values of apparent density, porosity and water absorption was carried out in accordance with [24].

The microhardness of the synthesized ceramics was determined by the Vickers method using a DuraScan-20 microhardness tester (EMCO-TEST, Austria). Test load – 2 kg, endurance at maximum load – 5 s.

The fracture toughness of ceramic materials was determined using the single edge V-notched beam (SEVNB) method in accordance with ISO 23146:2012. This standard specifies a method for the determination of the fracture toughness of advanced technical ceramics. The procedure uses the single-edge V-notched bars, which are loaded in four-point bending until failure. It is applicable to monolithic ceramics with a grain size or major microstructural feature size larger than about 1 μm. Rectangular bars with mechanically applied V-shaped stress concentrators were used as samples. The radius of curvature of the concentrators was ~7-9 μm. The samples were loaded according to a four-point bending scheme. Fracture toughness was assessed by a change in critical stress intensity factor (K1C) with increasing temperature.

The chemical composition was studied by X-ray fluorescence spectrometry on a portable X-ray analyzer S1 TITAN 600 (Bruker, USA). The microstructure of the samples was studied using a scanning electron microscope JSM-6390LV (JEOL, Japan).

3. Results and Discussion

According to the results of the study of the chemical composition of the obtained powder mixture by X-ray fluorescence spectrometry, zirconium (Zr) is proved to be the major component (Table 1). The chemical composition of the 6YSZ – Al_2O_3 – HfO_2 mixture is dominated by zirconium, with

Table 1 – X-ray fluorescence analysis of the chemical composition of 6YSZ – Al_2O_3 – HfO_2 powder

Chemical element	Content, %	Standard deviation
Zr	80.9783	0.5155
Al	8.7100	0.3873
Y	5.6983	0.1403
Hf	3.5266	0.4380
Fe	0.0181	0.0042
Ni	0.0162	0.0034
Cr	0.0152	0.0057
Zn	0.0193	0.0022

significant contributions from aluminum and yttrium, and a smaller yet substantial amount of hafnium. The low concentrations of minor elements and their higher relative variability suggest they are not primary constituents but could still impact the material properties. The combination of these elements is tailored to achieve a composite material with superior mechanical strength, thermal stability, and resistance to wear and cracking, making it suitable for demanding technological applications. Due to the lack of oxygen in the range of detectable elements of the X-ray analyzer, the content of it in the analyzed sample is not shown.

The size and surface morphology of the particles of the powder mixture 6YSZ – Al_2O_3 – HfO_2 are shown in Figure 1.

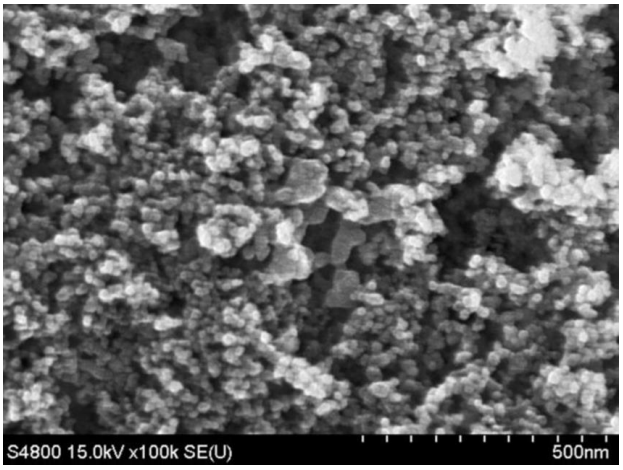

Figure 1 – Electronic image of particles of the powder mixture 6YSZ – Al_2O_3 – HfO_2

Figure 1 shows a distribution of fine particles with a high degree of uniformity in size. The particles appear to be mostly spherical or slightly angular, indicating a high level of homogeneity in shape. There are regions where particles appear to be clustered together, forming agglomerates. The agglomeration might be due to the intrinsic nature of nanopowders, which tend to cluster due to high surface energy and van der Waals forces. The particles exhibit a rough surface texture, which might be beneficial for sintering process as it can enhance particle bonding and densification. The powder mixture is well-dispersed overall, though there are a few denser clusters. The relatively uniform particle size and shape should contribute to a more homogeneous microstructure in the sintered ceramic, enhancing mechanical and thermal properties.

Figure 2 shows the change in the phase composition of the studied samples depending on the sintering temperature.

Miller indices indicating the transformation of a monoclinic lattice of zirconium oxide into a tetragonal one with the presence of a small amount of zirconium oxide with a monoclinic lattice were determined from the lines of diffractograms. The monoclinic crystalline structure of aluminum oxide has undergone transformation into hexagonal Al_2O_3. Y_2O_3 and HfO_2 are represented by monoclinic phases and have not undergone phase transformations in the studied temperature range. Thus, it was determined that after sintering the pressed samples in vacuum at 1400-1600°C, the crystal structure of the samples changes. In this case, the monoclinic structure was changed to a tetragonal one. As a result, a material similar in structure to tetragonal zirconium dioxide (TZP) was obtained, implemented in the 6YSZ – Al_2O_3 – HfO_2 system, mostly consisting of stabilized tetragonal structural elements [25, 26]. Temperature of 1600°C was considered to be the optimal temperature ensuring the highest yield of t-ZrO_2 phase.

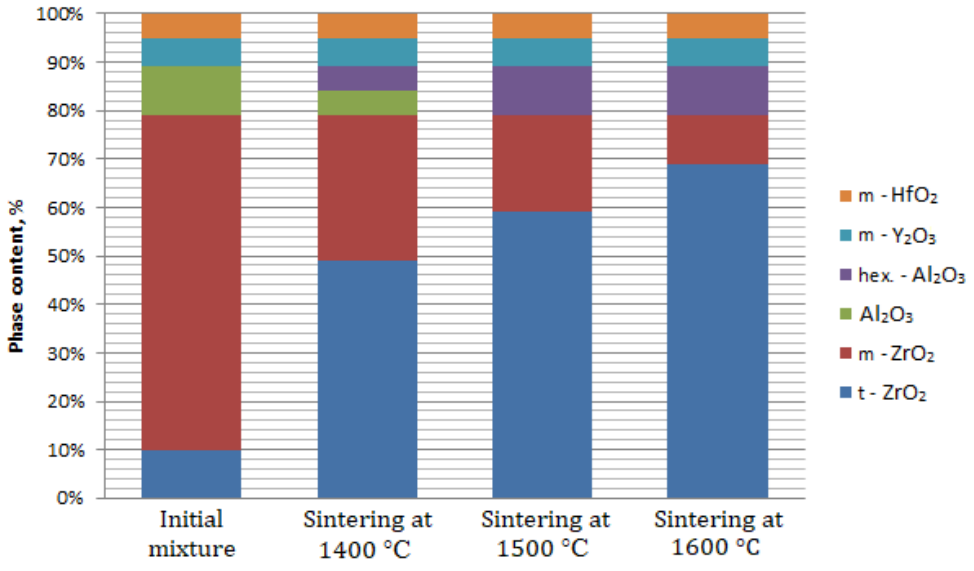

Figure 2 – Change in the phase composition of 6YSZ – Al_2O_3 – HfO_2 samples sintered at 1400, 1500, 1600°C

Figure 3 and Table 2 shows the results of X–ray phase analysis of samples synthesized from a powder mixture of 6YSZ – Al_2O_3 – HfO_2 sintered at a temperature of 1600°C.

The XRD pattern, with intensity plotted against the 2θ angle (in degrees, using Cu Kα radiation), reveals the presence of multiple crystalline phases. Tetragonal zirconium dioxide (t-ZrO_2) is prominently indicated by the intense peak at around 30°, which is the highest in the pattern, proving a significant presence of tetragonal zirconia in the sample. The presence of monoclinic zirconia is confirmed by several peaks at lower angles (approximately 20-35°). The presence of both tetragonal and monoclinic zirconia indicates a phase transformation that typically occurs in zirconium dioxide, influenced by the sintering temperature and conditions. Peaks corresponding to hexagonal alumina are observed, suggesting the integration of aluminum oxide within the sample matrix. This phase is significant in enhancing the material's thermal and mechanical properties. The identification of yttrium oxide peaks indicates its role as a stabilizer for zirconia phases, which is commonly used to maintain the tetragonal phase at room temperature. The presence of hafnium dioxide, a material with properties similar to zirconia, suggests its incorporation to potentially enhance the high-temperature stability and mechanical strength of the composite.

The presence of multiple zirconia phases (both tetragonal and monoclinic) alongside alumina, yttria, and hafnia suggests that the sample is a complex composite material. The high intensity of the tetragonal zirconia peak at around 30° indicates that this phase is predominant, which is desirable for applications requiring high fracture toughness and strength, as tetragonal zirconia is known for its transformation toughening mechanism.

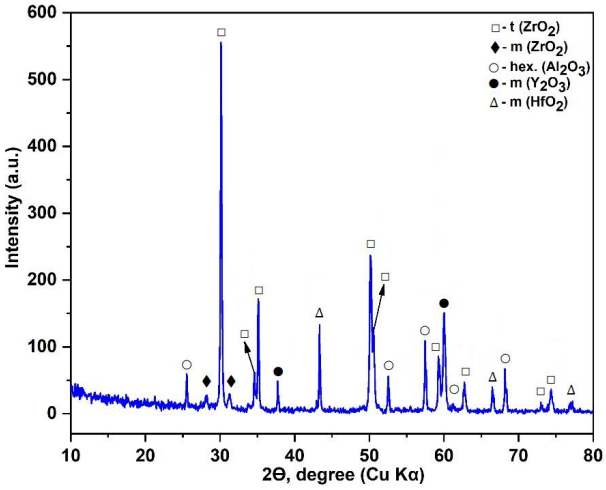

Figure 3 – X-ray diffraction (XRD) patterns of a sintered sample at T = 1600°C

The sintering process at 1600°C has effectively led to the formation of a composite material with a well-defined crystalline structure. The phase distribution suggests that careful control of the sintering parameters can tailor the material properties for specific applications.

We also conducted additional studies of the physico-mechanical properties of the obtained ceramic samples at the sintering temperature from 1400 to 1600°C. The results of the study of the physical and mechanical properties of ceramics are presented in Table 3.

Table 2 – Identification of phases on Figure 3

Phase	ICDD PDF card	Crystal structure	Space group	Lattice parameters			
				a	b	c	β
t-ZrO_2	01-079-1770	Tetragonal	P42/nmc (137)	3.596	3.596	5.183	
m-ZrO_2	01-083-0940	Monoclinic	P21/c (14)	5.145	5.207	5.311	99.2°
hex.-Al_2O_3	01-079-1557	Hexagonal	R-3c (167)	4.759		12.991	
m-Y_2O_3	00-025-1200	Monoclinic	C2/m (12)	7.599	6.616	7.906	104.0°
m-HfO_2	00-053-0560	Monoclinic	P21/c (14)	5.117	5.175	5.293	99.22°

Table 3 – Physical and mechanical properties of ceramics of the composition 6YSZ – Al_2O_3 – HfO_2

Sintering temperature, °C	Apparent density, g/cm³	Open porosity, %	Water absorption, %	Microhardness H_V, GPa
1400	5.4	0.31	0.09	11.2
1500	5.7	0.25	0.09	11.4
1600	5.8	0.19	0.07	12.1

The density of sintered ceramics made of partially stabilized ZrO_2 after heat treatment at 1400°C corresponds to a value of 5.4 g/cm^3 and acquires a maximum value at a firing temperature of 1600°C – 5.8 g/cm^3, which is 96% of the theoretical value. The density of the samples at a sintering temperature of 1500°C was 5.7 g/cm^3. That is, it can be seen that an increase in the sintering temperature entails an increase in the apparent density of the samples. Open porosity and water absorption values change proportionally to the sintering temperature of ceramics, the best characteristics of the values are observed at a sintering temperature of 1600°C. That is, an increase in the sintering temperature entails a decrease in porosity and water absorption. It was also established that as the sintering temperature increases, the microhardness of the obtained samples increases.

The change in the physico-mechanical properties of ceramic samples is associated with a corresponding change in the phase composition induced by temperature exposure, taking into account a certain stationary ratio of ceramic components. In addition, we assume that the presence of such a modifier as Al_2O_3 and HfO_2 in a powder mixture of zirconium dioxide in the form of a small concentration of about 5-6% made it possible to obtain materials containing almost 63% of tetragonal zirconium dioxide during sintering.

To achieve a relatively high level of strength of the resulting ceramics the following measures were taken: homogeneous distribution of oxides in an impeller-type reactor, compaction of samples and the use of dispersed systems [27, 28]. In this paper an assessment of the effect of the metastable state of zirconium dioxide on one of the important properties of ceramics - the crack resistance of the resulting material. The assessment of the resistance of materials to the nucleation and propagation of cracks was carried out using the SEVNB method. The results of the crack resistance measurement are shown in Figure 4. An increase in temperature to 1600°C leads to an increase in the level of K_{1C}, which correlates with the data of the maximum density at a given temperature. Of all the materials studied in the work, the highest values of crack resistance correspond to the material K_{1C} = 6.0 MPa√m sintered at a temperature of 1600°C. The resulting ceramics containing a metastable

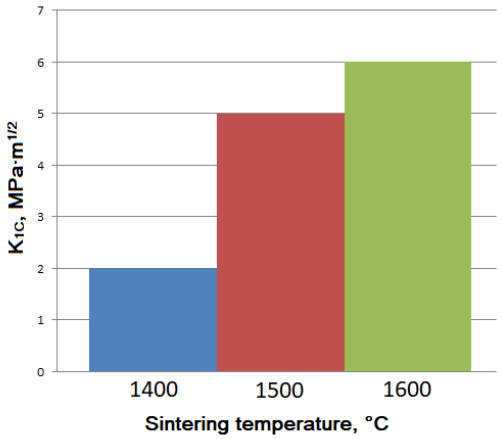

Figure 4 – Change in the critical stress intensity coefficient depending on the firing temperature of ceramics in the range 1400 – 1600°C

tetragonal phase of about 68% are characterized by the highest mechanical characteristics. Thus, temperature exposure is one of the ways to stabilize the tetragonal phase of zirconium dioxide.

The analysis of the microstructure of synthesized ceramics (Figure 5) indicates the absence of its sensitivity to the temperature regime of processing in the range 1400 – 1600°C. There is no clear grain boundary in the near-surface layers of ceramics. The microstructure of the sample sintered at 1400°C exhibits a dense and granular morphology, with small grains closely packed together. The grain size is relatively small, indicating that the sintering process has begun but is not yet fully complete, leading to a less coarsened structure. Compared to 1400°C, in the sample sintered at 1500°C the grains are slightly larger and more well-defined. The microstructure suggests increased grain growth and densification due to the higher sintering temperature, leading to a more uniform structure with fewer pores. As the temperature rises to 1600°C, ceramics reach a densely baked state without open porosity, while closed pores remain in the material.

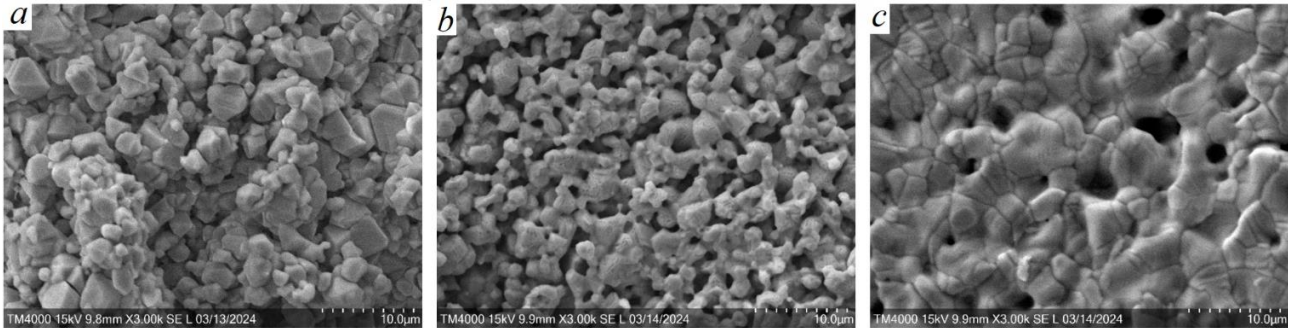

Figure 5 – SEM image of the microstructure of ceramics 6YSZ – Al_2O_3 – HfO_2 sintered in vacuum at 1400°C (a), 1500°C (b) and 1600°C (c)

The average grain size ranges from 1 to 7 microns. Due to the presence of a fine fraction in the form of flakes in the initial powder, for the formation of granules of the press mass, it became necessary to introduce a larger amount of organic binder – 10 wt.% (the optimal amount is up to 3 wt.%) which could also affect the formation of micropores.

The results of microanalysis of the polished surface of an experimental sample synthesized at a temperature of 1600°C are shown in Figure 6.

Figure 6 consists of two parts: (a) the micrography of the sample surface and (b) the corresponding spectral microanalysis. This figure provides both a visual representation of the sample's surface morphology and a quantitative analysis of its elemental composition. The surface exhibits a granular structure with closely packed particles. The uniformity in particle size and distribution indicates a homogeneous mixture of the components within the composite material. The particles appear to be fine, suggesting a high degree of sintering and particle bonding. This indicates a well-processed composite, leading to enhanced mechanical properties. The surface roughness is visible, which is typical for sintered ceramic materials. A significant peak for oxygen indicates its presence in all the oxides forming the composite, such as ZrO_2, Al_2O_3, and HfO_2. The dominant peak for zirconium confirms the major component of the composite as zirconia (ZrO_2), specifically the yttria-stabilized zirconia (YSZ) variant. A prominent peak for aluminum signifies the presence of aluminum oxide (Al_2O_3) within the composite. The peak for yttrium, although smaller compared to zirconium and aluminum, is crucial as it indicates the presence of yttria (Y_2O_3) to stabilize the zirconia phase, preventing the transformation from the tetragonal to monoclinic phase at room temperature. The hafnium peak, though less intense, confirms the incorporation of hafnium dioxide (HfO_2) in the composite. A small peak for carbon might be observed due to surface contamination or residue from the sample preparation process.

The homogeneous distribution of particles seen in the micrograph, along with the elemental analysis, indicates effective sintering and material processing. This uniformity is crucial for ensuring consistent material properties throughout the sample.

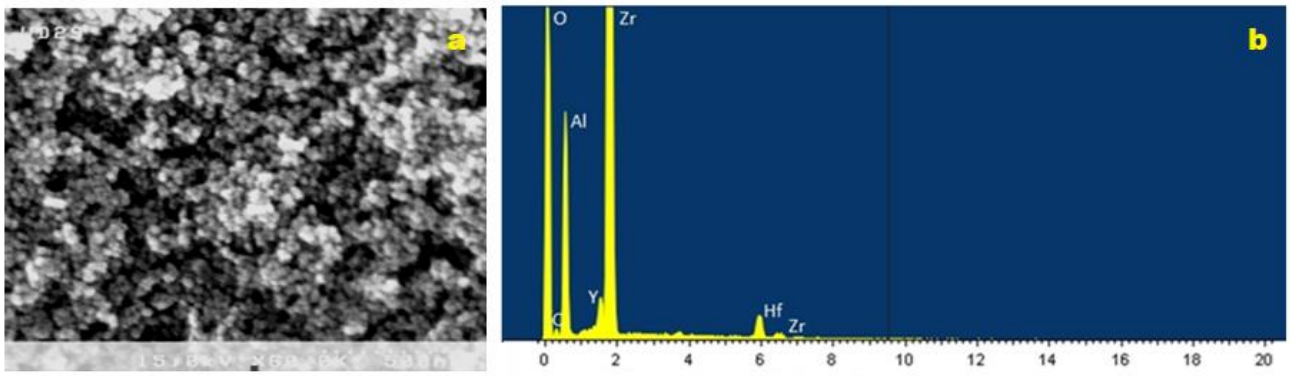

Figure 6 – Micrography of the surface of the sample 6YSZ – Al_2O_3 – HfO_2 (a) and spectral microanalysis (b)

4. Conclusion

The optimal composition of the powder mixture 6YSZ – Al_2O_3 – HfO_2 for vacuum sintering has been selected. Composite ceramics based on ZrO_2 were obtained through a step-by-step powder preparation process, including cavitation. The initial powder mainly consists of monoclinic zirconium dioxide, with small amounts of tetragonal ZrO_2, monoclinic aluminum oxide (Al_2O_3), Y_2O_3, and HfO_2, with an overall monoclinic phase composition of about 84%.

During sintering the ceramic samples containing 6YSZ, Al_2O_3, and HfO_2 at 1400-1600°C, monoclinic ZrO_2 transforms into tetragonal ZrO_2, with a small amount of monoclinic ZrO_2 remaining. The addition of monoclinic Al_2O_3 forms α-Al_2O_3 (corundum), a stable and densely packed structure. This results in a material similar to tetragonal zirconium dioxide (TZP), primarily consisting of stabilized tetragonal ZrO_2. Y_2O_3 and HfO_2 remain monoclinic and do not transform in the studied temperature range.

Physico-mechanical property studies show that the optimal vacuum sintering temperature for ceramic samples is 1600°C, achieving an apparent density of 5.8 g/cm^3 (96% of the theoretical value), with open porosity of 0.19%, water absorption of 0.07%, microhardness of 12.1 GPa, and crack resistance (K_{1C}) of 6.0 MPa·m$^{1/2}$. The stabilized ZrO_2 phase significantly contributes to the mechanical properties of the composite ceramics. Sintering stabilized tetragonal ZrO_2 results in high-density material, as the sintering temperature is mainly limited by the melting point.

The study highlights that temperature significantly affects the structure and physico-mechanical properties of ceramics synthesized from 6YSZ – Al_2O_3 – HfO_2 by semi-dry pressing and vacuum sintering. The developed oxide ceramic materials with high mechanical properties represent a significant advancement in materials science, offering potential for high-load applications.

Acknowledgements

This research was funded by the Science Committee of the Ministry of Science and Higher Education of the Republic of Kazakhstan, grant number AP19677974.

Authors' Contributions

M. Abilev: conceptualization, data curation, formal analysis, methodology, supervision, visualization, verification, writing – original draft, writing – review & editing; D. Yerbolat: conceptualization, data curation, formal analysis, methodology, visualization, writing – original draft, writing – review & editing; M. Skakov: conceptualization, data curation, formal analysis, methodology, project administration, resources, supervision, visualization, verification, writing – original draft, writing – review & editing; Al. Zhilkashinova: conceptualization, data curation, formal analysis, methodology, project administration, resources, software supervision, supervision, visualization, verification, writing – original draft, writing – review & editing; A. Pavlov: formal analysis, methodology, visualization, verification, writing – original draft, writing – review & editing; N. Kantay: conceptualization, formal analysis, visualization, verification, writing – original draft; S. Gert: conceptualization, formal analysis, visualization, verification, writing – original draft, writing – review & editing; As. Zhilkashinova: conceptualization, data curation, formal analysis, methodology, software supervision, supervision, visualization, verification, writing – original draft, writing – review & editing; L. Łatka: conceptualization, analysis, methodology, visualization, verification, writing – original draft, writing – review & editing.

References (GOST)

1 Dong X., An Q., Zhang S., Yu H., Wang M. Porous ceramics based on high-thermal-stability Al2O3–ZrO2 nanofibers for thermal insulation and sound absorption applications // Ceram Int. – 2023. – Vol.49, Is.19. – P.31035-31045.

2 Lu Y., Xie J., Guo Y., Liu C. Transparent magnesium aluminosilicate glass-ceramics with high content of ZrO2 // J Eur Ceram Soc. – 2024. – Vol.44, Is.15. – P.116721.

3 Wang H., Shen F., Li Z., Zhou B., Zhao P., et al. Preparation of high-performance ZrO2 bio-ceramics by stereolithography for dental restorations // Ceram Int. – 2023. – Vol.49, I.s17. – P.28048-28061.

4 Xiao Y., Zhu S., Duan J., Wang H., Huang Z., et al. Preparation and properties of Gd2O3–Eu2O3–ZrO2 ceramics as promising control rod material // Ceram Int. – 2023. – Vol.49, Is.23. – P.39458-39464.

5 Ghosh T.K., Chakrabarti S.K., Ghosh S., Saha S., Dey S., Das S.K. Synthesis, characterization, bioactivity and cytotoxicity assessment of nano ZrO2 reinforced bioactive glass ceramics // Ceram Int. – 2023. – Vol.49, Is.20. – P.32694-32710.

6 Song X., Ding Y., Zhang J., Jiang C., Liu Z., et al. Thermophysical and mechanical properties of cubic, tetragonal and monoclinic ZrO2 // J Mater Res Technol. – 2023. – Vol.23. – P.648-655.

7 Thakur M., Vij A., Singh F., Rangra V.S. Spectroscopic studies of metastable tetragonal ZrO2 nanocrystals // Spectrochim Acta A Mol Biomol Spectrosc. – 2024. – Vol.305. – P.123495.

8 Yurchenko Yu.V., Korniienko O.A., Bykov O.I., Samelyuk A.V., Yushkevych S.V., Zamula M.V. Phase equilibria in the ZrO2–HfO2–Nd2O3 system at 1500 °C and 1700 °C // Open Ceram. – 2023. – Vol.15. – P.100421.

9 Fábregas I.O., Craievich A.F., Fantini M.C.A., Millen R.P., Temperini M.L.A., Lamas D.G. Tetragonal-cubic phase boundary in nanocrystalline ZrO2–Y2O3 solid solutions synthesized by gel-combustion // J Alloys Compd. – 2011. – Vol.509. – P.5177-5182.

10 Zhu X., Hou G., Ma J., Zhang X., An Y., et al. Effect of Y2O3 doping content on phase composition, mechanical properties and cavitation erosion performance of ZrO2 ceramics // Ceram Int. – 2024. – Vol.50, Is.9. – P.14718-14730.

11 Jin E., Yuan L., Yu J., Ding D., Xiao G. Enhancement of thermal shock and slag corrosion resistance of MgO–ZrO2 ceramics by doping CeO2 // Ceram Int. – 2022. – Vol.48. – P.13987-13995.

12 Yurchenko Yu.V., Kornienko O.A., Olifan O.I., Sameliuk A.V., Yushkevych S.V., et al. Experimental study of isothermal sections of the ZrO2–HfO2–Eu2O3 ternary diagram at 1500 °C and 1700 °C // Calphad. – 2024. – Vol.86. – P.102721.

13 Sevastyanov V.G., Simonenko E.P., Simonenko N.P., Stolyarova V.L., Lopatin S.I., Kuznetsov N.T. Synthesis, vaporization and thermodynamics of ceramic powders based on the Y2O3–ZrO2–HfO2 system // Mater Chem Phys. – 2015. – Vol.153. – P.78-87.

14 Yu Z., Qi T., Ge M., Zhang W., Hu Z., Sun X. Microstructures and phase compositions of Y2O3–ZrO2–HfO2 solid solutions // Ceram Int. – 2023. – Vol.49. – P.26119-26128.

15 Du W., Ai Y., He W., Chen W., Liang B., Lv C. Formation and control of “intragranular” ZrO2 strengthened and toughened Al2O3 ceramics // Ceram Int. – 2020. – Vol.46. – P.8452-8461.

16 Sunil Kumar K., Suryaprakash Kalos P., Akhtar M.N., Shaik S., Sundara V., et al. Experimental and theoretical analysis of exhaust manifold by uncoated and coated ceramics (Al2O3, TiO2 and ZrO2) // Case Stud Therm Eng. – 2023. – Vol.50. – P.103465.

17 Dong X., An Q., Zhang S., Yu H., Wang M. Porous ceramics based on high-thermal-stability Al2O3–ZrO2 nanofibers for thermal insulation and sound absorption applications // Ceram Int. – 2023. – Vol.49. – P.31035-31045.

18 Choi J.-H., Nam M.-S., Ryu S.-S., Jung I.-H., Nahm S., Kim S. Thermodynamic stability and mechanical evaluation of YSZ-WC composite ceramics fabricated by pressureless sintering and hot pressing // Ceram Int. – 2023. – Vol.49, Is.9. – P.13414-13424.

19 Ramachandran K., Gnanasagaran C.L., Pazhani A., Kumar V.H., Xavior M.A., et al. Impact behaviour of MWCNTs reinforced YSZ and Al2O3 ceramic-nanocomposites prepared

via vacuum hot-pressing technique // J Mater Res Technol. – 2023. – Vol.24. – P.6595-6603.
20 Liu D., Fan J., Zhao K., Liu J., An L. Preparation of super-strong ZrO2 ceramics using dynamic hot forging // J Eur Ceram Soc. – 2023. – Vol.43, Is.2. – P.733-737.
21 Yu H., Chen Y., Guo X., Luo L., Li J., Li W., et al. Study on mechanical properties of hot pressing sintered mullite-ZrO2 composites with finite element method // Ceram Int. – 2018. – Vol.44, Is.7. – P.7509-7514.
22 Zhuiykov S. An investigation of conductivity, microstructure and stability of HfO2–ZrO2–Y2O3–Al2O3 electrolyte compositions for high-temperature oxygen measurement // J Eur Ceram Soc. – 2020. – Vol.20, Is.7. – P.967-976.
23 Maji A., Choubey G. Microstructure and mechanical properties of alumina toughened zirconia (ATZ) // Mater Today Proc. – 2018. – Vol.5, Is.2. – P.7457-7465.
24 GOST 2409-2014. Refractories. A method for determining apparent density, open, full and closed porosity and water absorption [Ogneupory. Metod opredeleniya kazhushcheysya plotnosti, otkrytoy i obshchey poristosti, vodopogloshcheniya]. – Intr. 2015-09-01. – Standardinform, Moscow, 2014. (In Russian)
25 Fu L., Li B., Xu G., Huang J., Engqvist H., Xia W. Size-driven phase transformation and microstructure evolution of ZrO2 nanocrystallites associated with thermal treatments // J Eur Ceram Soc. – 2021. – Vol.41, Is.11. – P.5624-5633.
26 Chen Y., Tan J., Sun J., Guo H., Bai J., Zhou P., et al. Effect of sintering temperature on the microstructures and mechanical properties of ZrO2 ceramics fabricated by additive manufacturing // Ceram Int. – 2024. – Vol.50, Is.7. – P.11392-11399.
27 Abilev M., Zhilkashinova A., Pavlov A., Zhambakin D., Tuyakbayev B. Structural-phase state and properties of SiC ceramics obtained by ultrasound-assisted liquid-phase sintering with eutectic additives // Silicon. – 2023. – Vol.15. – P.3921-3930.
28 Zhambakin D., Zhilkashinova A., Abilev M., Łatka L., Pavlov A., et al. Structure and properties of spark plasma sintered SiC ceramics with oxide additives // Crystals. – 2023. – Vol.13. – P.1103.

References

1 Dong X, An Q, Zhang S, Yu H, Wang M (2023) Ceram Int 49(19):31035-31045. *https://doi.org/10.1016/j.ceramint.2023.07.048*
2 Lu Y, Xie J, Guo Y, Liu C (2024) J Eur Ceram Soc 44(15):116721. *https://doi.org/10.1016/j.jeurceramsoc.2024.116721*
3 Wang H, Shen F, Li Z, Zhou B, Zhao P, e al (2023) Ceram Int 49(17):28048-28061. *https://doi.org/10.1016/j.ceramint.2023.06.052*
4 Xiao Y, Zhu S, Duan J, Wang H, Huang Z, et al (2023) Ceram Int 49(23):39458-39464. *https://doi.org/10.1016/j.ceramint.2023.09.291*
5 Ghosh TK, Chakrabarti SK, Ghosh S, Saha S, Dey S, Das SK (2023) Ceram Int 49(20):32694-32710. *https://doi.org/10.1016/j.ceramint.2023.07.237*
6 Song X, Ding Y, Zhang J, Jiang C, Liu Z, et al (2023) J Mater Res Technol 23:648-655. *https://doi.org/10.1016/j.jmrt.2023.01.040*
7 Thakur M, Vij A, Singh F, Rangra VS (2024) Spectrochim Acta A Mol Biomol Spectrosc 305:123495. *https://doi.org/10.1016/j.saa.2023.123495*
8 Yurchenko YuV, Korniienko OA, Bykov OI, Samelyuk AV, Yushkevych SV, Zamula MV (2023) Open Ceram 15:100421. *https://doi.org/10.1016/j.oceram.2023.100421*
9 Fábregas IO, Craievich AF, Fantini MCA, Millen RP, Temperini MLA, Lamas DG (2011) J Alloys Compd 509:5177-5182. *https://doi.org/10.1016/j.jallcom.2011.01.213*
10 Zhu X, Hou G, Ma J, Zhang X, An Y, et al (2024) Ceram Int 50(9):14718-14730. *https://doi.org/10.1016/j.ceramint.2024.01.385*
11 Jin E, Yuan L, Yu J, Ding D. Xiao G (2022) Ceram Int 48:13987-13995. *https://doi.org/10.1016/j.ceramint.2022.01.283*
12 Yurchenko YuV, Kornienko OA, Olifan OI, Sameliuk AV, Yushkevych SV, Zamula MV (2024) Calphad 86:102721. *https://doi.org/10.1016/j.calphad.2024.102721*
13 Sevastyanov VG, Simonenko EP, Simonenko NP, Stolyarova VL, Lopatin SI, Kuznetsov NT (2015) Mater Chem Phys 153:78-87. *https://doi.org/10.1016/j.matchemphys.2014.12.037*
14 Yu Z, Qi T, Ge M, Zhang W, Hu Z, Sun X (2023) Ceram Int 49:26119-26128. *https://doi.org/10.1016/j.ceramint.2023.05.168*
15 Du W, Ai Y, He W, Chen W, Liang B, Lv C (2020) Ceram Int 46:8452-8461. *https://doi.org/10.1016/j.ceramint.2019.12.080*
16 Sunil Kumar K, Suryaprakash Kalos P, Akhtar MN, Shaik S, Sundara V, et al (2023) Case Stud Therm Eng 50:103465. *https://doi.org/10.1016/j.csite.2023.103465*
17 Dong X, An Q, Zhang S, Yu H, Wang M (2023) Ceram Int 49:31035-31045. *https://doi.org/10.1016/j.ceramint.2023.07.048*
18 Choi JH, Nam MS, Ryu SS, Jung IH, Nahm S, Kim S (2023) Ceram Int 49(9):13414-13424. *https://doi.org/10.1016/j.ceramint.2022.12.216*
19 Ramachandran K, Gnanasagaran CL, Pazhani A, Kumar VH, Xavior MA, et al (2023) J Mater Res Technol 24:6595-6603. *https://doi.org/10.1016/j.jmrt.2023.04.199*
20 Liu D, Fan J, Zhao K, Liu J, An L (2023) J Eur Ceram Soc 43(2):733-737. *https://doi.org/10.1016/j.jeurceramsoc.2022.10.004*
21 Yu H, Chen Y., Guo X., Luo L., Li J., Li W., Xu Z., Li T., Wu G. (2018) Ceram Int 44(7):7509-7514. *https://doi.org/10.1016/j.ceramint.2018.01.146*
22 Zhuiykov S (2000) J Eur Ceram Soc 20(7):967-976. *https://doi.org/10.1016/S0955-2219(99)00233-2*
23 Maji A, Choubey G (2018) Mater Today Proc 5(2):7457-7465. *https://doi.org/10.1016/j.matpr.2017.11.417*
24 (2014) GOST 2409-2014. Refractories. A method for determining apparent density, open, full and closed porosity and water absorption [Ogneupory. Metod opredeleniya kazhushcheysya plotnosti, otkrytoy i obshchey poristosti, vodopogloshcheniya]. Standartinform, Moscow, Russia. (In Russian)

25 Fu L, Li B, Xu G, Huang J, Engqvist H, Xia W (2021) J Eur Ceram Soc 41(11):5624-5633. *https://doi.org/10.1016/j.jeurceramsoc.2021.04.058*

26 Chen Y, Tan J, Sun J, Guo H, Bai J, et al (2024) Ceram Int 50(7):11392-11399. *https://doi.org/10.1016/j.ceramint.2024.01.039*

27 Abilev M, Zhilkashinova A, Pavlov A, Zhambakin D, Tuyakbayev B (2023) Silicon 15:3921-3930. *https://doi.org/10.1007/s12633-023-02318-5*

28 Zhambakin D, Zhilkashinova A, Abilev M, Łatka L, Pavlov A, Tuyakbaev B, Zhilkashinova A (2023) Crystals 13:1103. *https://doi.org/10.3390/cryst13071103*

Information about authors

M. Abilev – PhD, associate professor of al-Farabi Kazakh National University, Almaty, Kazakhstan, Sarsen Amanzholov East Kazakhstan University, Ust-Kamenogorsk, Kazakhstan.

D. Yerbolat – Research Engineer of Center of Excellence VERITAS, Daulet Serikbaev East Kazakhstan Technical University, Ust-Kamenogorsk, Kazakhstan.

M. Skakov – Doctor of Physical and Mathematical Sciences, Professor, Academician of KazNAEN, Chief Researcher of National Nuclear Center, Professor of Sarsen Amanzholov East Kazakhstan University, Ust-Kamenogorsk, Kazakhstan.

Al. Zhilkashinova – Candidate of Physical and Mathematical Sciences, associate professor, leading researcher at the National scientific laboratory of Sarsen Amanzholov East Kazakhstan University, Ust-Kamenogorsk, Kazakhstan.

A. Pavlov – Candidate of Technical Sciences, S. Amanzholov East Kazakhstan University, "KAZCERAMICS" LLP, Director of Production at Scientific and Technical Center "Bakor", Ust-Kamenogorsk, Kazakhstan.

K. Nurgamit – PhD, Senior Researcher of Sarsen Amanzholov East Kazakhstan University, Ust-Kamenogorsk, Kazakhstan.

S. Gert – Master technologist of "KAZ CERAMICS" LLP, Master of Technical Sciences, Ust-Kamenogorsk, Kazakhstan.

As. Zhilkashinova – PhD, Senior Researcher of Sarsen Amanzholov East Kazakhstan University, Ust-Kamenogorsk, Kazakhstan.

L. Łatka – PhD (Eng.), DSc, Professor at Wroclaw University of Science and Technology, Wroclaw, Poland.